MASTER INTERNSHIP - PHYSICS
Nanosciences, Nanocomponents & Nanomeasures

The Internship Supervisor : Pr. Dr. BRITO Francisco de Assis
The Head of the Masters degree 3N : Pr. Dr. CORATGER Roland

Some Properties of Solids through q-Deformed Algebras

TRISTANT Damien

Contents

List of Figures

List of Tables

Acknowledgments

First and foremost, I would particularly like to thank my internship Director Prof. Dr. Francisco de Assis de Brito (Chico), researcher and teacher in charge of the Physics laboratory of the Federal University of Campina Grande, for his availability, his support, for being so open-minded, and without whom none of this work would not have been possible. These valuable advice helped me to carry out my end of Master 2, *Nanosciences, Nanocomponents & Nanomeasures*, in Brazil. In addition, I thank him for his patience, listen to student speaking "Portugenglish" it is not always easy!

My thanks also go to all the staff of the laboratory (students, researchers and teachers) who introduced me to the life of a scientific laboratory in Brazil and learned to celebrate São João around a glass of Cachaça ...

Thank you to the Senhora Nascimento Elizangela, student and president of "Centro Acadêmico de Físico" for her help and kindness. Her Trufas of Maracujá will remain impregnated in my stomach. I also thank Senhor Rodrigo Lima for unlocking my computer several times.

I would also like to thank and express my gratitude to a person who has become more than a friend, a real sister, Miss Poux Armelle. She knew during difficult times to support and encourage me. Beijos!

I thank my two teachers of Portuguese, Senhora Hortência Morais and Senhor Francinaldo de Souza Lima, for their patience and for teaching me, after hours and hours, to make the difference between Portuguese and Spanish.

A special thanks to two Brazilians who are dear to me. Senhora Anahi Castro for having hosted in her apartment and to be looked after me, like a mother, when I was sick. And Senhor Pedro Jorge Dantas de Carvalho, for introducing me to the Brazilian history and culture.

This long stay in Brazil would not have been possible without the help of our educational secretary of the University Paul Sabatier of Toulouse, Ms. Besombes Valerie. Not to mention, Prof. Dr. Bandeira Lucilene and Prof. Dr. Fossy Michel, professors and employees to Reitoria at the Federal University of Campina Grande.

I also thank the University Paul Sabatier of Toulouse for giving me a financial support.

A thank you to my brother Goulwenn, to have moved to the Brazilian Embassy in Paris, without whom I would not have got my Visa.

My final thoughts go to my family, my mother Marie-Andrée and my father Pierrick.

Abbreviation

We show here, abbreviations and constant values that we used to perform our numerical calculations.

C_{v_q} q-deformed specific heat $(J\,mol^{-1}K^{-1})$

C_{ve_q} q-deformed electronic specific heat $(J\,mol^{-1}K^{-1})$

ε_F Fermi energy (J)

γ_q Sommerfeld parameter $(mJ\,mol^{-1}K^{-2})$

h Planck constant : $6.63 \cdot 10^{-34}Js$

$\hbar$ Reduced Planck constant : $\frac{h}{2\pi} = 1.05 \cdot 10^{-34}Js$

k_B Boltzmann constant : $1.38 \cdot 10^{-23}JK^{-1}$

m_e Mass of the electron : $9.10 \cdot 10^{-31}kg$

N_A Avogadro constant : $6.02 \cdot 10^{-23}mol^{-1}$

Θ_{D_q} The q-deformed Debye temperature (K)

T_F Fermi temperature (K)

T_f Melting temperature (K)

T_q Critical temperature (K)

T_{0_q} Separation temperature electron/phonon (K)

Introduction

Used for the first time by the mathematician Vladimir Drinfeld in the reference to deformed Hopf algebras [1], the study of quantum groups has attracted great interest in recent years, stimulating intense research in different fields of physics, taking into account a wide range of applications, ranging from the study of the fractional quantum Hall effect, black holes and high-Tc superconductors, to the non-commutative geometry, quantum theory of super-algebra and so on.

All current proposals for quantum groups suggest the idea of classical deformation of an object, which can be, for example, an algebraic group or a Lie group, knowing that the deformed objects lose their group properties. The concept of quantum groups was motivated by problems from a large number of physical situations, and with this understanding, led to ideas that motivated the theory.

In a study conducted in 1904, Frank Hilton Jackson introduces an element called the q-deformed algebra [2]. He used a q-analog theorem or expression, which is a generalization involving a new parameter, denoted q, having the property to return the original theorem or expression when selected its limiting case when q tends to 1 [3]. The q-deformed oscillators are derived from Jackson derivate q-operators, which are considered to define a q-deformed generalized dynamics in the q-commutative phase space. To do this one, we use the creation and annihilation operators of the q-deformed quantum mechanics.

The motivation of our study lies in the fact that a full understanding of the physical origin of the q-deformation of classical physics is still lacking. It is not clear that there is a standard answer to the q-deformation mechanics inspired by the study of quantum groups. But appeared recently great interest investigating the q-deformed thermodynamic systems at classical level. Deformed theory manages the statistical behavior of complex systems whose underlying dynamics is calibrated on an area of multi-fractal phase governed by the long-range interaction and the effects of long-term memory [4].

A mechanism capable of generating a deformed version of the classical statistical mechanics is to replace the Boltzmann-Gibbs distribution by its deformed version. In this sense, it is postulated a form of entropy that involves a deformed theory of generalized thermodynamics. Thus, some generalizations of statistical mechanics have been proposed [5]. In this context, it was shown that a natural realization of q-deformed thermodynamics bosons and fermions can be built on the "q-calculus" formalism.

In the recent past, some developing in q-deformed quantum group were studied [6]. In a specific case, we focus our attention on the study of the thermal and electrical problem in a solid.

A solid consists of a large number of atoms linked by cohesive forces of various kinds. Atomic

motion in a solid is very slight, causing every atom to move only within a small neighborhood, and vibrate around its equilibrium point. In a crystalline solid, the equilibrium points of atomic vibrations form a regular spatial structure, such as a cubic or hexagonal structure. Interaction between atoms allows the propagation of elastic waves in solid media, which can be both horizontal and longitudinal. Although this phenomenon is predominant at room temperature, it is very different at low temperature, where the electronic part take a more important role. Previous studies have analyzed the behavior of the q-deformed phonon contribution [7].

In this report, we are going to add the q-deformed electronic contribution and discuss new properties and obtained parameters.

In the first part, we present a brief introduction of the q-deformed quantum algebra, with the creation and annihilation operators. Then in a second part, we set up our fermionic system by calculating the q-deformed Fermi-Dirac statistics. In the third part, we use this statistics to get some q-deformed thermodynamic parameters (the q-deformed total energy, specific heat, Sommerfeld parameter,etc.), where we note that the q-deformation can be a phenomena due to impurities in the material. Finally, we present our conclusions and ongoing research.

All calculations and graphs were performed thanks to the software *MAPLE 16*.

Chapter 1

The q-deformed quantum algebra

It is necessary to first perform a general construction of the algebra of q-deformed operators.

The q-deformed algebra of the quantum oscillator is defined by q-deformed Heisenberg algebra in terms of creation operator $\hat{a}^\dagger$, annihilation operator $\hat{a}$ and the quantum number $\hat{N}$, by [8]

$$\left[\hat{N}, \hat{a}^\dagger\right] = \hat{a}^\dagger, \qquad \left[\hat{N}, \hat{a}\right] = -\hat{a}, \tag{1.1}$$

and

$$\hat{a}^\dagger \hat{a} = \left[\hat{N}\right], \qquad \hat{a}\hat{a}^\dagger = \left[1 - \hat{N}\right]. \tag{1.2}$$

The q-Fock space spanned by orthornormalized eigenstates $|n\rangle$ is constructed according to

$$|n\rangle = \frac{\left(\hat{a}^\dagger\right)^n}{\sqrt{[n]!}} |0\rangle, \qquad a|0\rangle = 0. \tag{1.3}$$

The action of $\hat{a}$, $\hat{a}^\dagger$ and $\hat{N}$ on the states $|n\rangle$ in the q-Fock space are known to be

$$\hat{a}|n\rangle = \sqrt{[n]} |n - 1\rangle, \tag{1.4}$$

$$\hat{a}^\dagger |n\rangle = \sqrt{[1 - n]} |n + 1\rangle, \tag{1.5}$$

$$\hat{N}|n\rangle = n|n\rangle. \tag{1.6}$$

We have the basic q-deformed quantum number $[x]$ is defined as [9]

$$[x] \equiv \frac{q^x - q^{-x}}{q - q^{-1}}, \tag{1.7}$$

where q is an arbitrary real number, $0 < q < \infty$, but the formulation is symmetric and can be limited to cases $0 < q < 1$ or $1 < q < \infty$, defined by a symmetry $q \to q^{-1}$ and the observed value of q has to satisfy the non-additivity [10]

$$[x + y] \neq [x] + [y]. \tag{1.8}$$

At limit $q \to 1$, the basic q-deformed quantum number $[x]$ is reduced to the number x and we find the classical physical properties of materials. The Pauli exclusion principle is also applicable for the q-deformed fermions, the eigenvalues of the number operator $\hat{N}$ can only be taken the values of $n = 0$ and 1.

The case study of fermionic is mainly due to expression (1.2), by using the Poisson brackets

$$\hat{a}\hat{a}^{\dagger} = \left[1 - \hat{N}\right],$$ (1.9)

and the Pauli exclusion principle. If we were to study the bosonic case, it is necessary to replace the previous equation by

$$\hat{a}\hat{a}^{\dagger} = \left[1 + \hat{N}\right].$$ (1.10)

Having laid the foundation for our q-deformed quantum development, we seek to express the q-deformed Fermi-Dirac statistics used in statistical physics.

Chapter 2

The q-deformed Fermi-Dirac statistics

To calculate the mean occupation numbers (q-deformed Fermi-Dirac statistics) of each energy level, we choose the Hamiltonian of non-interacting q-deformed fermions [11]

$$\hat{H} = \sum_{\theta} \left(\varepsilon_{\theta} - \mu \right) \hat{N}_{\theta}, \tag{2.1}$$

where $\hat{N}_{\theta}$ and ε_{θ}, are respectively the number operator and energy associated with the state label θ, and μ is the chemical potential of the system.

The main value of the q-deformed occupation number $f_{\theta,q}$ is defined by :

$$[f_{\theta,q}] = \frac{1}{\Xi} tr(\exp(-\beta\hat{H}) [N_{\theta}]), \tag{2.2}$$

where $\Xi = tr(\exp(-\beta\hat{H}))$ is the partition function, where $\beta = 1/(k_B T)$, k_B is the Boltzmann constant. So we find

$$[f_{\theta,q}] = \frac{1}{tr(\exp(-\beta\hat{H}))} tr(\exp(-\beta\hat{H})a_{\theta}^{\dagger}a_{\theta}). \tag{2.3}$$

Thanks to the cyclic properties of the trace [12], and using the above equations (1.2),(1.6) and (2.1), we can get

$$[f_{\theta,q}] = \frac{\exp(-\beta\hat{H})}{tr(\exp(-\beta\hat{H}))} tr(\exp(-\beta\hat{H})a_{\theta}a_{\theta}^{\dagger}), \tag{2.4}$$

$$[f_{\theta,q}] = \exp(-\beta\hat{H}) \frac{tr(\exp(-\beta\hat{H}) [1 - N_{\theta}])}{tr(\exp(-\beta\hat{H}))}, \tag{2.5}$$

$$[f_{\theta,q}] = \exp(-\beta\hat{H}) [1 - f_{\theta,q}], \tag{2.6}$$

$$\frac{[f_{\theta,q}]}{[1 - f_{\theta,q}]} = \exp(-\beta(\varepsilon_{\theta} - \mu)). \tag{2.7}$$

Using the definition of q-deformed number $[x]$,

$$\frac{[f_{\theta,q}]}{[1 - f_{\theta,q}]} = \frac{q^{f_{\theta,q}} - q^{-f_{\theta,q}}}{q^{1-f_{\theta,q}} - q^{f_{\theta,q}-1}} = \exp\left(-\beta\left(\varepsilon_\theta - \mu\right)\right). \tag{2.8}$$

the final solution is defined by

$$f_{\theta,q} = \frac{1}{2\ln(q)} \ln\left(\frac{q + \exp\left(\beta\left(\varepsilon_\theta - \mu\right)\right)}{q^{-1} + \exp\left(\beta\left(\varepsilon_\theta - \mu\right)\right)}\right). \tag{2.9}$$
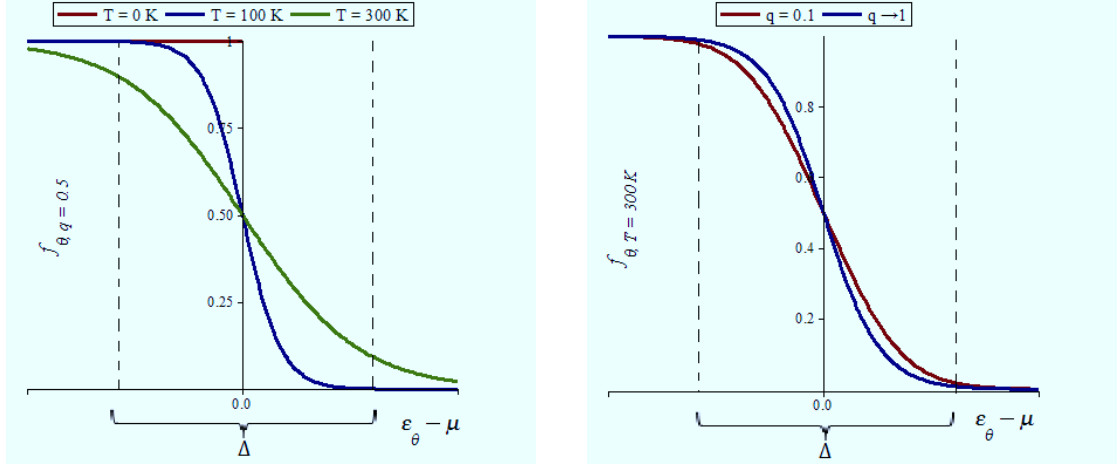
Figure 2.1: We plot the function of q-deformed occupation number (2.9), left figure, for different temperatures ($T = 0K$, $100K$ and $300K$) and a value of $q = 0.5$ and right figure, for different q-deformed ($q = 0.1$ and 1) and $T = 300K$.

At limit $q \to 1$, the q-deformed occupation number $[f_{\theta,q}]$ is reduced to the Fermi-Dirac distribution, $f_\theta = 1/(\exp(\beta(\varepsilon_\theta - \mu)) + 1)$. We get the same properties as a function of the Fermi-Dirac distribution, i.e., at absolute zero kelvin, the probability is equal one for energies less than the Fermi energy and zero for energies greater than the Fermi energy. Moreover, whatever the value of the temperature, $f_\theta = 0.5$ when $\varepsilon_\theta = \mu$.

On the right Fig.2.1, the decrease in the value q reduces the inclination of the slope of the q-deformed Fermi-Dirac function ($q \propto 1/T$). We can compare this phenomenon in the classical case when the tempertaure is increased. Moreover, whatever the value of q-parameter, the interval Δ is proportional to the temperature.

We note that the q-deformed Fermi-Dirac statistics differs significantly from the q-deformed Bose-Einstein distribution [13], which is given by equation

$$n_{\theta,q} = \frac{1}{\ln(q)} \ln\left(\frac{\exp\left(\beta\left(\varepsilon_\theta - \mu\right)\right) - 1}{\exp\left(\beta\left(\varepsilon_\theta - \mu\right)\right) - q}\right). \tag{2.10}$$

14

Chapter 3

Implementation of the q-deformation

We consider an ideal gas of q-fermions confined in a three-dimensional box. The electrons move in a constant effective potential, which results from the interaction of the electron mean made out off all other electrons and ions.

The q-deformed total number of particules and the q-deformed total energy of the system can be, respectively, expressed as

$$N_q\left(T\right) = \int_0^\infty \mathrm{d}E \, g(E) f_{\theta,q}(E,T), \tag{3.1}$$

$$U_q\left(T\right) = \int_0^\infty \mathrm{d}E \, g(E) f_{\theta,q}(E,T)E, \tag{3.2}$$

where, in three dimensions, the function of density states[1] $g(E)$ is proportional to $\sqrt{E}$.

These integrals are of the type, $\int_0^\infty \mathrm{d}E \, h(E) f_{\theta,q}(E,T)$. They can be evaluated by noting that $f_{\theta,q}(E,T)$ is evolving rapidly around $E = \mu$, when $T \ll T_F$. Using the integration by parts

$$\int_0^\infty \mathrm{d}E \, h(E) f_{\theta,q}(E,T) = [H(E) f_{\theta,q}(E,T)]_0^\infty - \int_0^\infty \mathrm{d}E \, H(E) \frac{\partial f_{\theta,q}(E,T)}{\partial E}, \tag{3.3}$$

where

$$H(E) = \int_0^E h(E) dE. \tag{3.4}$$

At limit $E \to \infty$, $H(E) f_{\theta,q}(E,T)$ tends to 0 : $f_{\theta,q}(E,T)$ tends to 0 more rapidly than $H(E)$ tends to infinity, because $H(E)$ is of the form $g(E)$ and $g(E)E$, these functions do not grow exponentially. Then $H(E = 0) = 0$, and taking into account the fact that $\frac{\partial f_{\theta,q}(E,T)}{\partial E}$ is practically zero for $E < 0$, so we can write (3.3) equal to

$$\int_0^\infty \mathrm{d}E \, h(E) f_{\theta,q}(E,T) = - \int_0^\infty \mathrm{d}E \, H(E) \frac{\partial f_{\theta,q}(E,T)}{\partial E}. \tag{3.5}$$

If $H(E)$ does not vary too rapidly in the neighborhood of $E = \mu$, it can be developed in Taylor series $H(E)$ and keep the first three terms of the development

---

[1]The density of states depends on a constant $C = \frac{1}{2\pi^2}\left(\frac{2m_e}{\hbar^2}\right)^{3/2}$ related to the mass of the electron m_e.

$$H(E) = H(\mu) + (E - \mu)\left(\frac{\partial H(E)}{\partial E}\right)_{E=\mu} + \frac{1}{2}(E - \mu)^2\left(\frac{\partial^2 H(E)}{\partial E^2}\right)_{E=\mu}, \qquad (3.6)$$

By substituting the equation (3.6) in the expression (3.5), we get

$$\int_0^\infty dE\, h(E) f_{\theta,q}(E, T) = -H(\mu)\int_0^\infty dE\, \frac{\partial f_{\theta,q}(E, T)}{\partial E}$$
$$-\left(\frac{\partial H(E)}{\partial E}\right)_{E=\mu}\int_0^\infty dE\,(E - \mu)\frac{\partial f_{\theta,q}(E, T)}{\partial E} - \frac{1}{2}\left(\frac{\partial^2 H(E)}{\partial E^2}\right)_{E=\mu}\int_0^\infty dE\,(E - \mu)^2\frac{\partial f_{\theta,q}(E, T)}{\partial E}.$$
$$(3.7)$$

Realizing a change of variables for the function $f_{\theta,q}$, with $x = \beta(E - \mu)$ and $dx = dE\,\beta$. The lower bound of the integrals can be replaced by $-\infty$ at low temperatures, and using the equation (3.4) we obtain

$$\int_0^\infty dE\, h(E) f_{\theta,q}(E, T) = -\int_0^\mu dE\, h(E)\int_{-\infty}^\infty dx\, \frac{\partial f_{x,q}}{\partial x} - h(E = \mu)\frac{1}{\beta}\int_{-\infty}^\infty dx\, x\frac{\partial f_{x,q}}{\partial x}$$
$$-\left(\frac{\partial h(E)}{\partial E}\right)_{E=\mu}\frac{1}{2\beta^2}\int_{-\infty}^\infty dx\, x^2\frac{\partial f_{x,q}}{\partial x}, \quad (3.8)$$

where

$$\frac{\partial f_{x,q}}{\partial x} = \frac{1}{2\ln(q)}\left(\frac{1}{1 + q\exp(x)} - \frac{1}{1 + q^{-1}\exp(x)}\right). \qquad (3.9)$$

Equation (3.8) is composed of three terms. Whatever the value of q, in the first term, the integral equals -1; in the second term, the integral equals 0, because the function is odd; only the third term depends on the q-deformation, where the integral is negative (see Appendix graphs 5).

We put for the continuation of our calculations the integral

$$\int_{-\infty}^\infty dx\, x^2\frac{\partial f_{x,q}}{\partial x} = I(q). \qquad (3.10)$$

Table 3.1 shows some solutions of the integral (3.10) for different values of q. We use this information a little later in our calculations.

Now, we can use equation (3.8) to obtain the q-deformed thermodynamic quantities.

3.1 The q-deformed total number of particles and chemical potential

The q-deformed number of particules is defined by

q	$I(q)$	q	$I(q)$	q	$I(q)$
0.05	-6.2813	0.40	-3.5697	0.75	-3.3174
0.10	-5.0571	0.45	-3.5024	0.80	-3.3064
0.15	-4.4895	0.50	-3.4500	0.85	-3.2986
0.20	-4.1532	0.55	-3.4090	0.90	-3.2935
0.25	-3.9304	0.60	-3.3768	0.95	-3.2907
0.30	-3.7730	0.65	-3.3517	$\to 1$	-3.2898
0.35	-3.6572	0.70	-3.3322		

Table 3.1: This table shows different values of the integral (3.10) calculated with some values of q. The graph of this function is represented in the Appendix Figure 6.

$$N_q(T) = \int_0^\infty dE\, g(E) f_{\theta,q}(E,T). \tag{3.11}$$

Using the equations (3.8), (3.10) and (3.11) with $h(E) = C\sqrt{E}$, we get the q-deformed total number of particules equation $N_q(T)$, depending of the chemical potential $\mu_q(T)$

$$N_q(T) = C\left(\frac{2}{3}\mu_q(T)^{3/2} - \frac{1}{4\beta^2}\mu_q(T)^{-1/2} I(q)\right). \tag{3.12}$$

The variation of the chemical potential $\mu_q(T)$ is obtained by noting that the electron density $N_q(T)$ is constant when the temperature varies

$$N_q(T=0) = N_q(T \neq 0). \tag{3.13}$$

We noted previously, when the temperature is zero, the q-deformed Fermi-Dirac statistics $f_{x,q} = 1$, so the q-deformed total number of particles $N_q(T)$ is defined by

$$N_q(T=0) = \int_0^{\varepsilon_F} g(E) dE, \tag{3.14}$$

so,

$$\int_0^{\varepsilon_F} dE\, \sqrt{E} = \int_0^\mu dE\, \sqrt{E} - \frac{1}{2\beta^2}\left(\frac{\partial\sqrt{E}}{\partial E}\right)_{E=\mu} I(q), \tag{3.15}$$

$$\int_\mu^{\varepsilon_F} dE\, \sqrt{E} = -\frac{1}{2\beta^2}\left(\frac{\partial\sqrt{E}}{\partial E}\right)_{E=\mu} I(q). \tag{3.16}$$

The term $\int_\mu^{\varepsilon_F} dE\, \sqrt{E}$, takes important values for energies close to the Fermi level ε_F. Noting that the Fermi temperature $T_F = \varepsilon_F/k_B$, in the case of free electron gas in three dimensions, the expression of the q-deformed chemical potential is given by

$$\mu_q(T) = \varepsilon_F\left(1 + \left(\frac{T}{2T_F}\right)^2 I(q)\right). \tag{3.17}$$

Let us note that $\mu_q(T)$ differs from ε_F by low terms (T^2). One replaces μ in Eq.(3.8) using Eq.(3.17). Notice that μ appears as a limit of integration (expand to first order in $\mu - \varepsilon_F$. Then, we rewrite the expression (3.8)

$$\int_0^\infty \mathrm{d}E\, h(E) f_{\theta,q}(E,T) = \int_0^{\varepsilon_F} \mathrm{d}E\, h(E) - (\varepsilon_F - \mu) h(\varepsilon_F) - \frac{1}{2\beta^2} \left(\frac{\partial h(E)}{\partial E}\right)_{E=\varepsilon_F} I(q). \quad (3.18)$$

3.2 The q-deformed total energy of the system and specific heat of the electron gas

The q-deformed total energy of the system is defined by

$$U_q(T) = \int_0^\infty \mathrm{d}E\, g(E) f_{\theta,q}(E,T) E. \quad (3.19)$$

Using the equations (3.18) and (3.19) with $h(E) = CE\sqrt{E}$ and the expression of the q-deformed chemical potential (3.17), we get the q-deformed total energy of the system

$$U_q(T) = C\varepsilon_F^{5/2} \left(\frac{2}{5} - \frac{1}{2}\left(\frac{T}{T_F}\right)^2 I(q)\right). \quad (3.20)$$

We note that the q-deformed total energy of the system depends only on Fermi temperature and q-deformed parameter inclued in the integral $I(q)$.

The q-deformed electronic specific heat $C_{Ve_q}(T)$ is defined by

$$C_{Ve_q}(T) = \left(\frac{\partial U_q(T)}{\partial T}\right)_V. \quad (3.21)$$

Differentiating equation (3.20), relative to T, we obtain

$$C_{Ve_q}(T) = -C\varepsilon_F^{5/2} \frac{T}{T_F^2} I(q). \quad (3.22)$$

But we can simplify this last equation, using the following expressions, $C = (2m_e/\hbar^2)^{3/2}/(2\pi^2)$, $\varepsilon_F = \hbar^2 k_F^2/(2m_e)$ and $T_F = \varepsilon_F/k_B$. Where k_F is the Fermi wave vector. Inserting these equations in the expression (3.22), using N_A, Avogadro constant and noting $n = N/V = k_F^3/(3\pi^2)$ the electronic density, we obtain our final equation of the q-deformed electronic specific heat

$$C_{Ve_q}(T) = -\frac{3}{2}nk_B N_A \frac{T}{T_F} I(q). \quad (3.23)$$

At limit $q \to 1$, the q-deformed electronic specific heat $C_{Ve_q}(T)$ is reduced to the classic electronic specific heat [14]

$$C_{Ve}(T) = \frac{\pi^2}{2}nk_B N_A \frac{T}{T_F}. \quad (3.24)$$

18

We note, that by comparing this result with the specific heat of an ideal gas [15] $\frac{3}{2}nk_BN_A$, the effect of q-deformed occupation number (whatever the value of q) is to reduce the q-deformed electronic specific heat by a factor of $-TI(q)/T_F$. At room temperature $(300K)$ and whatever the value of $q \in [0.1;1]$, it is of the order of $[10^{-1};10^{-2}]$. This explains why we do not detect a significant contribution of the q-deformed electronic specific heat at room temperature. However, it is interesting to study some metals (eg. alloys) at low temperatures, because they provide electrical and thermal properties (eg. superconductivity) different from the room temperature.

From Eq.(3.23), we can write the q-deformed electronic specific heat as the product of a variable, Sommerfeld parameter γ_q (depending on the q-deformed parameter) and temperature

$$C_{Ve_q}(T) = \gamma_q T, \tag{3.25}$$

where the Sommerfeld parameter is

$$\gamma_q = -\frac{3}{2}\frac{nk_BN_A}{T_F}I(q). \tag{3.26}$$

The Table 3.2 below compares the calculated values of $\gamma_{q\to1}$ (free-electrons) with experimental values. This comparison requires some foresight. The specific heat of a metal contains two major parts. At room temperature, a solid absorbs heat mainly through the vibrations of ions about their equilibrium positions. However, these contributions vanish as T^3 at low temperatures. There is a linear contribution (if the value of the q-deformed parameter is fixed) of the specific heat from the electrons. Experimental data support this claim. The authors of these references have multiplied the Eq.(3.26) (q tends to 1), by the volume and by the number of conduction electrons Z. In addition, this Table 3.2 allows you to verify our calculations, $\gamma_{q\to1}$, listed in the Table 3.3. Indeed, when the value of the q-parameter tends to 1, we find the same theoretical values and that for many metals.

Metal	Z	γ (mJ mole^{-1} K^{-2})		Metal	Z	γ (mJ mole^{-1} K^{-2})	
		Expt.	Eq. (6.78)			Expt.	Eq. (6.78)
Li	1	1.65	0.74	Al	3	1.35	0.91
Na	1	1.38	1.09	Ga	3	0.60	1.02
K	1	2.08	1.67	In	3	1.66	1.23
Rb	1	2.63	1.90	Sn	4	1.78	1.41
Cs	1	3.97	2.22	Pb	4	2.99	1.50
Cu	1	0.69	0.50	Sb	5	0.12	1.61
Ag	1	0.64	0.64	Bi	5	0.008	1.79
Au	1	0.69	0.64	Mn	2	12.8	1.10
Be	2	0.17	0.5	Fe	2	4.90	1.06
Mg	2	1.6	0.99	UPt$_3$		450	
Ca	2	2.73	1.51	UBe$_{13}$		1100	
Sr	2	3.64	1.79				
Ba	2	2.7	1.92				
Zn	2	0.64	0.75				
Cd	2	0.69	0.95				

Experimental results are obtained from an extrapolation to low temperatures assuming that $c_V/T \sim \gamma + \beta T^2$, as in Figure 13.10. The theoretical estimate uses electron densities n from Table 6.1. Data are presented for metals for which the comparison is fairly successful, for several metals for which it fails noticeably, and for heavy-fermion compounds for which it fails spectacularly. Source: Stewart (1983), and Stewart (1984).

Metal	Valence	Free-electron γ (10^{-3} J mole^{-1}K^{-2})	Experimental γ (10^{-3} J mole^{-1} K^{-2})
Na	1	1.09	1.7
K	1	1.67	1.7
Ag	1	0.64	0.66
Au	1	0.64	0.67
Cu	1	0.50	0.69
Ba	2	1.95	2.72
Ca	2	1.51	2.72
Sr	2	1.80	3.64
Co	2	0.61	4.98
Fe	2	0.64	5.02
Ni	2	0.61	7.02
Al	3	0.91	1.30
Ga	3	1.02	0.63
Sn	4	1.39	1.84
Pb	4	1.50	2.93
As	5	1.30	–
Sb	5	1.63	0.628
Bi	5	1.79	0.08

Table 3.2: Table left [16] and right [17], comparison of experimental [18] and calculated (free-electron) values of the Sommerfeld parameter γ for selected metals. Although this left table is used in many articles in physics, it is important to note here, there is an error on the theoretical value of iron γ. It is for this reason that I compare my $\gamma_{q\to1}$ values using two different references.

To understand the effects of q-deformation on the Sommerfeld parameter, it is necessary and interesting to plot, for some metals, γ_q function of q. Data is plotted to provide a better view of our results. For illustration purposes, we chose aluminum (Al), copper (Cu), iron (Fe), three materials that can be employed in many areas of interest and bismuth (Bi), gold (Au) and silver (Ag).

The Fig.3.1 shows how q-deformation acts on these materials Sommerfeld parameter. We plot in 'dotted' our theoretical data (where the shape of the function is $|q|^{-1}$) obtained from Eq.(3.26)[2], then full line, experimental data.
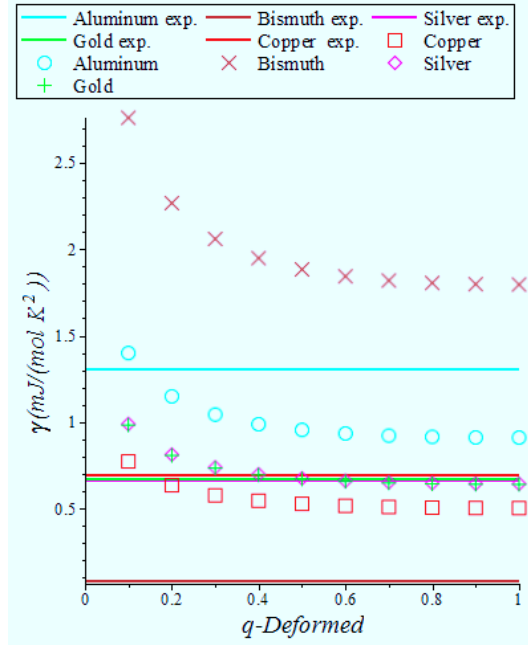

Figure 3.1: The q-deformed Sommerfeld parameter theory (dashed curves) and experimental (line) as a function of parameter $0 < q < 1$ for several metals, aluminum, gold, bismuth, silver and copper.

The plots, Fig.3.2, show that Cu reaches Ag experimental value for $q \approx 0.17$, while Ag approaches Au experimental value for $q \approx 0.53$. For copper (Cu), at limit $q \to 1$, the theoretical value is equal to the experimental value when $q \approx 0.15$. Thus, by varying the value of q of a chemical element, one modifies the Sommerfeld parameter until the physical properties of another chemical element. This one, amounts to modifying the Fermi energy (depends of the Fermi temperature) and therefore to vary the number of electrons per unit volume n. For example, Fig.3.2, when we vary $Cu(q \to 1)$ until $Cu(q \approx 0.17) = Ag$ exp., we decreases the number of electrons per unit volume in the copper. But if we vary $Ag(q \to 1)$ until $Ag(q \approx 0.53) = Au$ exp., we increases the number of electrons per unit of volume in the silver[3].

---

[2]Multiplied by the volume and by the number of conduction electrons to match the data from Table 3.2.

[3]The number of electrons per unit of volume or conduction electron density for gold $n_{Au} = 5.90 \cdot 10^{22} cm^{-3}$, silver $n_{Ag} = 5.86 \cdot 10^{22} cm^{-3}$ and copper $n_{Cu} = 8.49 \cdot 10^{22} cm^{-3}$ are given in Table.6.1 in reference[19].
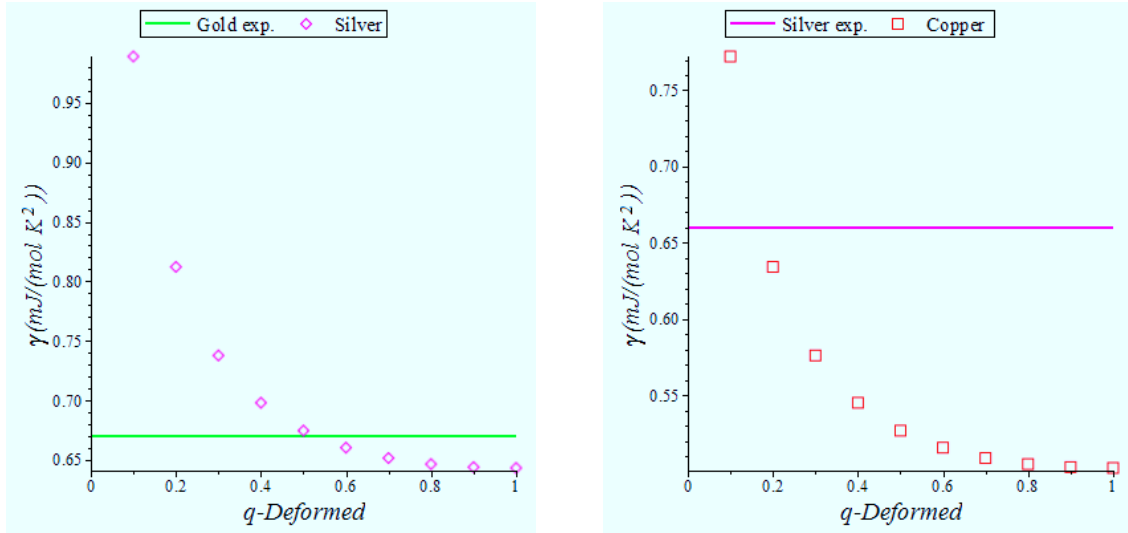
Figure 3.2: The q-deformed Sommerfeld parameter theory (dashed curve) and experimental (line) as a function of parameter $0 < q < 1$. On the left figure, the experimental value of gold and theoretical values of silver. On the right figure, the experimental value of silver and the theoretical values of copper.

Copper is one of the best electrical conductors for which the method of free electrons is appropriate. Indeed, from Fig.3.3, where $q \approx 0.15$, the theoretical value of copper is in agreement with the experimental value. But there are metals in the periodic table to which the estimate of the free electrons of the specific heat is seriously in error, such as iron. According to our results, when $q \approx 2.6 \cdot 10^{-4}$, the theoretical value of iron equals the experimental value.

We need to return in 1964 to understand why there is such a large gap between $\gamma_{q \to 1}$ and $\gamma_{exp.}$ iron. Indeed the physicist J. Kondo, assumes the presence of magnetic impurities screened by clouds of electrons. These clouds of electrons have the effect of diffusing the conduction electrons, thereby increasing the resistance [20]. This behavior turns out to be related to the presence of magnetic impurities in a metal and involves the process where an electron leaves the impurity to be replaced by another electron, which can be of opposite spin (turnaround spin of impurity). This effect is emphasized through the q-deformation, since the significant intervention of impurities lowers the value of the parameter q-deformed.
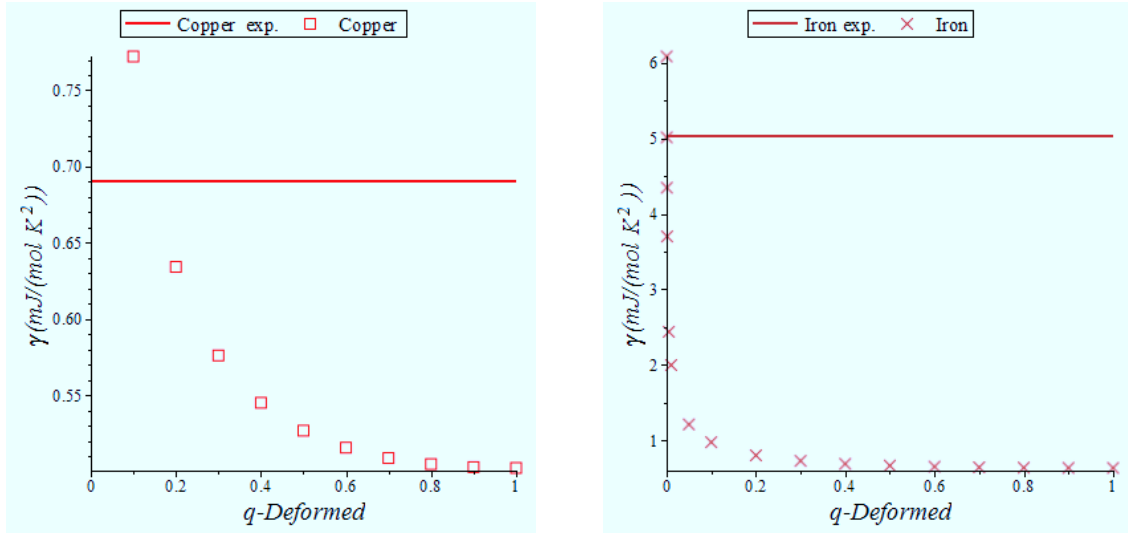
Figure 3.3: The q-deformed Sommerfeld parameter theory (dashed curves) and experimental (line) as a function of parameter $0 < q < 1$ for the copper (left figure) and for the iron (right figure).

3.3 The q-deformed total specific heat

As we saw above, the electronic contribution to the q-deformed specific heat is greater than the contribution of phonons at low temperatures. It is well known [21], that the specific heat of a metal C_V (electronic and phonons contribution), contains two major parts, low and high temperature[4]. The same goes for the q-deformed specific heat

$$C_{V_q}(T) = C_{VD_q}(T) + C_{Ve_q}(T). \tag{3.27}$$

The first term in Eq.(3.27) represents the q-deformed Debye specific heat, obtained by A.A. Marinho, F.A. Brito and C. Chesman [7], using the Debye's model[5]. It treats the vibration of the atomic lattice, i.e. phonons in the box

$$C_{VD_q}(T) = 3k_B N_A \left(-\frac{3\left(\frac{\Theta_{D_q}}{T}\right)}{\exp\left(\frac{\Theta_{D_q}}{T}\right) - 1} + \frac{12}{\left(\frac{\Theta_{D_q}}{T}\right)^3} \int_0^{\frac{\Theta_{D_q}}{T}} d\alpha \frac{\alpha^3}{\exp(\alpha) - 1} \right), \tag{3.28}$$

where Θ_{D_q} is the q-deformed Debye temperature. Table 3.3 shows some values of Θ_{D_q} for different values of q and different metals [7]. By adding the second term, q-deformed electronic specific heat previously calculated, we obtain the expression of the q-deformed specific heat

---

[4]It is considered at low temperatures, the temperatures below the Debye temperature, $T \ll \Theta_D$ and high temperatures, the temperatures above the Debye temperature, $T \gg \Theta_D$.

[5]All the oscillators do not vibrate at the same frequency ω.

$$C_{V_q}(T) = 3k_B N_A \left(-\frac{3\left(\frac{\Theta_{D_q}}{T}\right)}{\exp\left(\frac{\Theta_{D_q}}{T}\right) - 1} + \frac{12}{\left(\frac{\Theta_{D_q}}{T}\right)^3} \int_0^{\frac{\Theta_{D_q}}{T}} d\alpha \, \frac{\alpha^3}{\exp(\alpha) - 1} \right) + \gamma_q T. \qquad (3.29)$$

When the temperature is high in comparison with all the phonon frequencies $(T \gg \Theta_{D_q})$, i.e., when all normal mode is in a highly excited state, then the arguments in the exponential are low, the function $C_{VD_q}(T)$ can be expressed in a Taylor series in $\frac{\Theta_{D_q}}{T}$

$$C_{VD_q}(T) = 3k_B N_A \left(1 - \frac{\left(\frac{\Theta_{D_q}}{T}\right)^2}{20} \right). \qquad (3.30)$$

In addition, we have seen previously, the term containing the Sommerfeld parameter is small at high temperatures. Thus, when the temperature tends to infinity, we obtain the following equation

$$C_{V_q}(T) = 3k_B N_A. \qquad (3.31)$$

So we get the Dulong-Petit law [22], which depends neither the temperature nor the parameter q-deformed. At very low temperatures $(T \ll \Theta_{D_q})$, we can write the Eq.(3.29) as

$$C_{V_q}(T) = \frac{12\pi^4 k_B N_a}{5} \left(\frac{T}{\Theta_{D_q}} \right)^3 + \gamma_q T. \qquad (3.32)$$

Thus, as in the usual Debye solid, low temperature q-deformed Debye and the electronic specific heat is proportional respectively to T^3 and T. By studying the q-deformed case at low and high temperatures, we find the same properties of the classical specific heat.

It is useful to have a measure of the temperature at which the specific heat of a metal is no longer dominated by the electronic contribution rather than the contribution of lattice vibrations. Dividing Eq.(3.25)[6] by the expression at low temperatures of the contribution of phonons, this temperature T_{0_q} is obtained

$$T_{0_q} = \frac{1}{2\pi^2} \sqrt{-\frac{5nI(q)\Theta_{D_q}^3 Z}{2T_F}}. \qquad (3.33)$$

The Fermi temperature is very large relative to the q-deformed Debye temperature. T_{0_q} is typically a few Kelvin. This explains why the linear term in the q-deformed specific heat is observed only at low temperatures. The variation of the parameter q, for example copper, $T_{0_{q \to 1}} = 3.22K$, $T_{0_{q=0.5}} = 3.30K$ and $T_{0_{q=0.1}} = 4.00K$, increases the temperature. This result agrees with the observation made previously in chapter 3 (the right Fig.2.1). Thus, when the q-parameter decrease the temperature T_{0_q} increases from a few percent.

---

[6]Multiplied by the number of conduction electrons Z.

For the q-deformed case we can observe the changes that occur with Debye temperature, Sommerfeld parameter γ and total specific heat. See Table 3.3 below for room temperature $T = 300K$.

Element	$T_F^{(a)}$ (10^4)	$\Theta_{D_q}^{(b)}$			$\gamma_q^{(c)}$			$C_{V_q}^{(d)}$		
		$q{=}0.1$	$q{=}0.5$	$q{\to}1$	$q{=}0.1$	$q{=}0.5$	$q{\to}1$	$q{=}0.1$	$q{=}0.5$	$q{\to}1$
Cs	1.76	44.5	38.6	38	3.58	2.44	2.33	25.99	25.66	25.62
Rb	2.06	65.5	56.8	56	3.06	2.08	1.99	25.80	25.53	25.50
K	2.37	106.5	92.4	91	2.66	1.81	1.73	25.59	25.37	25.35
Pb	10.97	122.9	106.6	105	2.30	1.56	1.49	25.43	25.26	25.24
Ba	4.22	128.7	111.6	110	2.98	2.03	1.94	25.61	25.38	25.36
Bi	11.43	139.3	120.8	119	2.75	1.88	1.79	25.51	25.31	25.29
Na	3.66	184.9	160.4	158	1.72	1.17	1.12	24.99	24.95	24.94
Au	6.42	193.1	167.4	165	0.98	0.67	0.64	24.73	24.76	24.76
Sn	11.86	234.1	203	200	2.12	1.45	1.38	24.84	24.82	24.81
Cd	8.66	244.6	212.1	209	1.45	0.99	0.95	24.57	24.63	24.63
Ag	6.38	263.3	228.4	225	0.98	0.67	0.64	24.31	24.44	24.45
Ca	5.48	269.2	233.5	230	2.30	1.57	1.49	24.66	24.68	24.68
Ga	12.11	374.5	324.8	320	1.56	1.06	1.01	23.57	23.86	23.89
Zn	10.93	382.7	332	327	1.15	0.78	0.75	23.37	23.72	23.75
Cu	8.17	401.4	348.2	343	0.77	0.52	0.50	23.08	23.50	23.54
Li	5.43	402.6	349.2	344	1.16	0.79	0.75	23.18	23.57	23.60
Al	13.53	500.1	434.4	428	1.39	0.95	0.91	22.21	22.80	22.85
Fe	12.94	550	477	470	0.97	0.66	0.63	21.50	22.25	22.32
Be	16.67	1685.2	1461.7	1440	0.75	0.51	0.49	7.74	9.73	9.95

Table 3.3: Chemical elements and their respective Fermi temperature ^{a} (K) [14], Debye temperatures ^{b} (K) [7], Sommerfeld parameter γ_q ^{c} $(\frac{mJ}{mol \cdot K^2})$, Total specific heat ^{d} $(\frac{J}{mol \cdot K})$, for $T = 300K$ and their deformations for $q = 0.1$ and $q = 0.5$.

Thereafter, we plot (Fig.3.4) the q-deformed specific heat (taking into account the term of the Debye and Sommerfeld) depending on the temperature, for three values of $q \in \{0.1; 0.5; 1\}$, and for two different materials, copper (Cu) and cesium (Cs). First, we note that the curves when the temperature is very low, varies T^3. Then when the temperature increases, we note that the values of C_{V_q} for $q \in \{0.1; 0.5\}$, are lower than the values of $C_{V_{q \to 1}}$, up to a certain value of temperature, noted T_q and we call critical temperature. Beyond this temperature, the C_{V_q} values for $q \neq 1$ diverge and do not respect the Dulong-Petit law.

To understand this phenomenon, we must analyse the q-deformed specific heat curves for copper and cesium at high temperatures, i.e., above the critical temperature of copper and cesium which are respectively, $T_{q_{Cu}} \approx 576.9K$ and $T_{q_{Cs}} \approx 83.3K$. Our physical study, in the case of solid, stops from the melting temperature of Cu and Cs which are respectively $T_{f_{Cu}} = 1357.77K$ and $T_{f_{Cs}} = 301.65K$ [23].
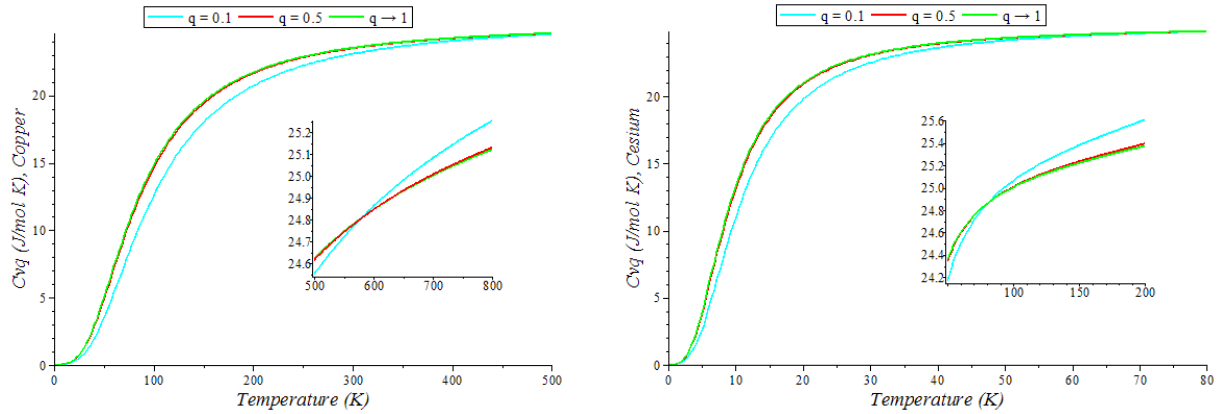
Figure 3.4: The q-deformed specific heat as a function of temperature for $q = 0.1$, $q = 0.5$ and $q \to 1$, for copper (left figure) and cesium (right figure).

Indeed, above the critical temperature, $C_{V_{q \neq 1}}(T)$ values continue to grow. There is a major reason for this phenomenon. According to the Kopp-Neumann law, the specific heat of solid chemical combinations is equal to the sum of the specific heats of pure elements. For example, at $800K$, the specific heat of the CuO is 54 J/(mol.K) [24]. This explains why $C_{V_{q \neq 1}}(T)$ values do not stabilize around a constant as predicted by the Dulong-Petit law.

If we follow this reasoning, when the value of q decreases, it means we added a new compound in the pure element (here copper) and then added some impurities. This joined the conclusion of previous work (Sommerfeld parameter), to show that the q-deformed algebra acts as a factor of disorder or impurity.

Thereafter, it would be useful to analyze experimentally the physical effect which is at the critical temperature T_q (which matches neither the Fermi temperature nor the q-deformed temperature Debye), where the curves cross at a single point. Nevertheless, we observe, for Cu and Cs that the critical temperature occurs at around 24.85 J/(mol.K), the value close to that predicted by Dulong-Petit law (25 J/(mol.K)).

Conclusion and Perspective

In this report, we studied the electronic contribution together with the contribution of phonons [7] in the limit of low and high temperatures by applying a q-deformation. The application of the q-deformed in these well-known problems have resulted in a better understanding of the q-deformation.

We obtain theoretically results of q-deformed to the number of particules, the total energy of the system, the chemical potential and the specific heat. The latter is the more interesting because it allows us to obtain, with simple parameters (Sommerfeld parameter, temperature), some information about the properties of the q-deformed solid. At limit $q \to 1$, we find that the results are identical to the classical case referenced in the literature.

Until now, obtaining the specific heat (phonons) the thermal and electrical conductivity have shown some q-deformed solid Einsten or Debye properties. The electronic contribution, allowed us to obtain the q-deformed Sommerfeld parameter. Preliminary results on this parameter shows that some metals have the same characteristics q-deformed than others. For example, copper Cu, has the same characteristics as silver Ag when $q \approx 0.17$. In addition, we find that this parameter γ_q is linked to the number of electrons per unit volume. This changes when q varies.

Although some metals do not follow the method of free electrons, for example iron, q-deformation can still get good results. Indeed, it highlights the involvement of impurities, reducing the parameter q-deformed. We support this result through the Kondo theory, which predicts the magnetic impurities intervention in some metals, such as iron. So, the q-deformation (here formulated with the free electrons) helps to explain physical phenomenons which are traditionally decried by more sophisticated methods such as the Kondo's method.

By adding the electrons contribution to the phonons contribution, we obtain the q-deformed total specific heat. At low temperature, the temperature T_{0_q} separating the main contribution of electrons and phonons is shifted to higher temperatures gradually when the q-deformed factor decreases. For example, for copper Cu, the temperature increase of 20% if $q = 0.1$. At high temperature, while the classic case follows the Dulong-Petit law, the values q-deformed, eg. $q = 0.1$, diverge from a certain critical temperature T_q. This phenomenon can be explained by the Kopp-Neumann law. According to this law, our metal is not pure and consists of new elements that we can associate with impurities.

In future work, it would be interesting to analyze more precisely the physical effect that occurs when we reach the critical temperature T_q, which matches neither the Fermi temperature nor the q-deformed temperature Debye.

Thus, we see the possibility of applying the q-deformed on different models, acting as a factor of disorder or impurity. We believe that these defects are mainly due to the factor of

doping, i.e., the addition of impurities or defects (donors or acceptors of elecrons), which greatly affects the electronic properties of metals. But we still need to analyze other characteristics of metals to establish more precisely the results through the q-deformation.

Thanks to this new study, this report comes support and enrich the previous assumptions found in the literature, and shows that the q-deformation also acts on the electrons. Nowadays, researchers try to link this theory with experiments, for example the growth of thin films, to better understand the q-deformation.

Brazil is a country primarily known for the cheerfulness of its people, football and samba. But in recent years, shows have acquired a great potential in the field of sciences and technologies, especially in that of modern physics (condensed matter, string theory).

My stay in Brazil, especially in the north, in the city of Campina Grande has therefore not restricted to my research laboratory.

At first, I focused my attention on learning Portuguese.

Then I had the opportunity to deepen my knowledge by working at the *Museu Vivo de Ciência e Tecnologia e Inovação Lynaldo Cavalcanti* from Campina Grande, to rehabilitate the experiments in classical and modern physics and teaching in Portuguese, electrical energy to high school students.

Later, I had the chance to get for one semester, a federal teaching position at the Federal University of Campina Grande. Where I have a responsibility to teach in Portuguese, electromagnetism (courses and practical work) to undergraduate students.

My research had led by the submission of a scientific paper and a seminar I conducted in English. In this report, I presented one part of my research, the second part concerns the q-deformed superconductivity which is in progress. My internship in Brazil will conclude in August by the validation of my master in Brazil (dissertation and presentation of my research in Portuguese).

Bibliography

[1] J. Fuchs, Affine Lie Algebras and Quantum Groups, Cambridge University Press (1992).

[2] F.H. Jackson, Proc. Edin. Math. Soc. 22, 28-39 (1904).

[3] B.E. Palladino and P.L. Ferreira, RBEF 21,4 (1999).

[4] A. Lavagno, A.M. Scarfone and P.N. Swamy, J. Phys. A. Math. Theor. **40**, 8635-8654 (2007).

[5] S. Abe, Phys. Lett. A **224**, 326 (1997).

[6] G. Bimonte, C. Esposito, G. Marmo and C. Stornaiolo, Phys. Lett. A **318**, 313 (2003).

[7] A.A. Marinho, F.A. Brito and C. Chesman, Thermal properties of a solid through q-deformed algebra, Physica A **391**, 3424 (2012).

[8] J.J. Sakurai, Modern Quantum Mechanics, Late-Univ. of California, LA (1985).

[9] T. Ernst, The History of q-calculus and a new method. (Dep. Math., Uppsala Univ.) (1999-2000).

[10] C. Tsallis, Introduction to Nonextensive Statistical Mechanics, New York (2009).

[11] J.A. Tuszynski, J.L. Rubin, J. Meyer and M. Kibler, Phys. Lett. A **175** (1993).

[12] Lee C R and Yu J P, Phys. Lett. A **150**, 63 (1990).

[13] A. Lavagno and P. Narayana Swamy, Thermostatistics of a q-deformed boson gas (2000).

[14] M. P. Marder, Condensed Matter Physics, Corrected Printing (2000).

[15] G. Faverjon, Thermodynamique PCSI, Breal (2003).

[16] M. P. Marder, Condensed Matter Physics, Corrected Printing, p.151 (Table 6.2) (2000).

[17] T. M. Tritt, Thermal Conductivity : Theory, Properties and Applications (2004).

[18] N. W. Aschroft and N. D. Mermin, Solid state physics (Sounders, Philadelphia) (1976).

[19] M. P. Marder, Condensed Matter Physics, Corrected Printing, p.147 (Table 6.1) (2000).

[20] J. Kondo, Resistance Minimum in Dilute magnetic alloys, Prog. Theor. Phys. 32, 37 (1964).

[21] C. Kittel, Solid State Physics (1995).

[22] E.A. Guggenheim, Thermodynamique, Dunod (1965).

[23] D.R. Lide, Handbook of chemistry and physics, CRC, Press Inc. (2009).

[24] F. Seitz, The modern theory of solids, McGraw-Hill, New York, USA (1940).

.1 Appendix

In this appendix we show graphs to better visualize the functions and check for some values of q if the main shape of these functions are preserved.
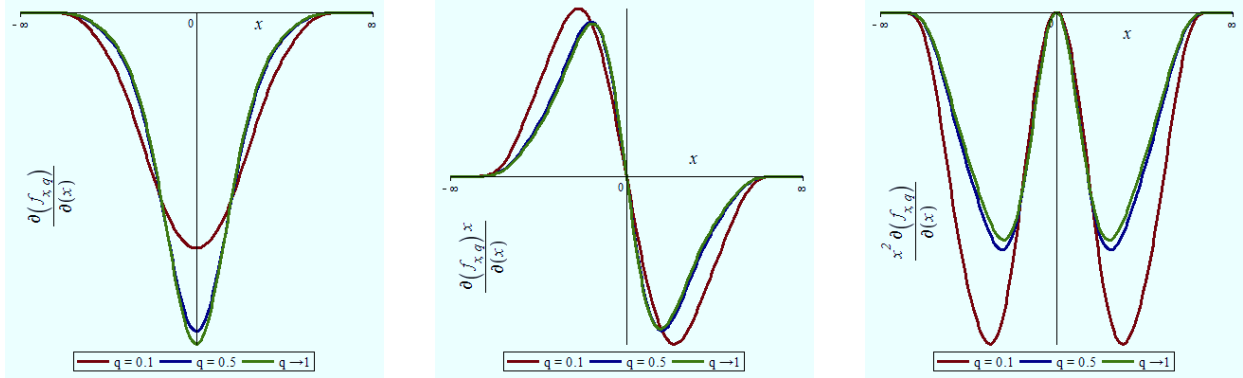

Figure 5: Representation of the different functions of Eq.(3.8), from left to right for $\frac{\partial f(x,q)}{\partial x}$, $x\frac{\partial f(x,q)}{\partial x}$ and $x^2\frac{\partial f(x,q)}{\partial x}$, where $\frac{\partial f(x,q)}{\partial x}$ is developed in the Eq.(3.9), for $q = 0.1$, $q = 0.5$ and $q \to 1$. Show that there are solutions to the converging values. Note, the functions of the left and right figures are evens and those of the central figure are odd (i.e. the integral is zero), which facilitates the calculations.
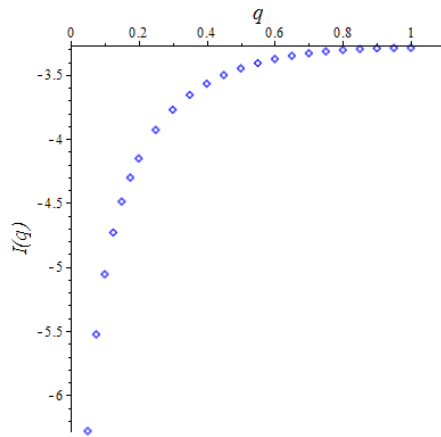

Figure 6: We represent some of the values of the function $I(q)$, Eq.(3.10). We note that it evolves in $-q^{-1}$, which will have a substantial and significant effect in our equations.